ASTRONOMY & ASTROPHYSICS
SUPPLEMENT SERIES

Astron. Astrophys. Suppl. Ser. **130**, 207–214 (1998)

Far-infrared emission from Shakhbazian Compact Galaxy Groups⋆

H.M. Tovmassian[1], J.M. Mazzarella[2], G.H. Tovmassian[3], D. Stoll[4], and H. Tiersch[4]

[1] Instituto Nacional de Astrofísica Optica y Electrónica, AP 51 y 216, 72000, Puebla, Pue., México
e-mail: hrant@inaoep.mx
[2] MS 100-22, IPAC, California Institute of Technology, Jet Propulsion Laboratory, Pasadena, CA 91125, U.S.A.
[3] Observatorio Astronómico Nacional, Instituto de Astronomía, UNAM, AP 877, 22860, Ensenada, B.C., México
[4] Sternwarte Königsleiten, München, Germany

Received November 18, 1997; accepted December 04, 1997

Abstract. Using the IRAS archives, we searched for far-infrared (FIR) counterparts of Shakhbazian Compact Groups of Galaxies (SCGGs). Reliable IRAS detections are identified at the positions of 24 out of 367 SCGGs; another 10 IRAS sources, located within ~ 2 arcmin of SCGGs, are possibly associated with the corresponding galaxy groups. Some of these sources are not very reliable. Previous work has shown that the fraction of E and S0 galaxies in a representative sample of SCGGs is 77%, while E and S0 galaxies comprise about 51% of galaxies in Hickson Compact Groups (HCGs). The higher fraction of early Hubble types, combined with their greater distances, explains the low IRAS detection rate of SCGGs ($7-8$%) compared to HCGs (64%). The FIR colors and morphological types of galaxies in the groups suggest that active star formation or Seyfert galaxies may be the main source of the FIR emission in the SCGGs detected by IRAS, perhaps originating as the result of tidal interactions in the dense environments of these groups.

Key words: infrared: galaxies — galaxies: interactions

1. Introduction

It is widely accepted that collisions or tidal interactions between galaxies may trigger bursts of star formation (e.g., Joseph & Wright 1985; Bushouse 1987; Norman 1988; Laurikainen & Moles 1989). One manifestation is often far-infrared (FIR) radiation which is enhanced in comparison with isolated galaxies of comparable optical luminosity. Indeed, as shown by Sanders et al. 1988, luminous infrared galaxies with $L_{\rm fir} > 10^{11} L_{\odot}$ are nearly all interacting or merging systems with exceptionally luminous nuclei. Optical spectra of such galaxies indicate a mixture of starbursts and active galactic nuclei (e.g., Veilleux et al. 1995).

In dense galaxy cluster environments, such as systems of compact groups of galaxies, tidal interactions between galaxies are expected to occur frequently. Hence galaxy groups provide a unique environment for testing theories of star formation triggered by tidal interactions, and to search for enhanced FIR dust emission. The most well known compact groups are the Hickson's (1982) Compact Groups (HCGs), which have been studied extensively (e.g., Pildis et al. 1995, and references therein). Hickson et al. (1989) inspected the IRAS Point Source Catalog (PSC) and detected emission at 60 μm and 100 μm from 54 galaxies in 45 out of 100 groups. They concluded that the FIR fluxes of galaxies in these groups are enhanced by about a factor of 2 compared to a sample of isolated galaxies. Sulentic & De Mello Rabaça (1993) reconsidered the problem and showed that the conclusion of Hickson et al. on the enhanced FIR fluxes was somewhat overestimated because the large IRAS beam encompassed the emission from more than one galaxy in many groups. In follow-up work, Allam et al. (1996) used the HIRAS software based on the Pyramid Maximum Entropy Method (Bontekoe et al. 1994) to partially resolve the component galaxies. They detected at 60 μm 87 individual sources in 62 HCGs out of 97 observed. Thus an appreciable number of galaxies in Hickson's compact groups are FIR sources.

Another interesting, but less well known sample is the Shakhbazian Compact Groups of Galaxies (SCGGs) (Shakhbazian 1973; Shakhbazian & Petrosian 1974; Baier et al. 1974; Petrosian 1974, 1978; Baier & Tiersch 1975, 1976a,b, 1978, 1979). These groups are more dense formations than Hickson's groups, with angular sizes typically of the order of $2-3$ arcmin. The distances between

Send offprint requests to: H.M. Tovmassian
⋆ Figures 2 and 3 only available in the online version at http://www.edpsciences.com

galaxies in SCGGs are $3-5$ times the diameter of a typical member galaxy, and the density of galaxies in the groups approaches $10^3 - 10^4$ Mpc^{-3}. Hence these groups are very compact. An investigation of the axial ratios of the SCGGs (Oleak et al. 1995) showed that these systems are usually highly flattened, with a prolate spheroidal shape ("cigars"). Each SCGG consists typically of 5–15 members. The apparent magnitude of member galaxies ranges approximately from $14^{\rm m}$ to $19^{\rm m}$. Almost all galaxies in the groups appeared very red on the POSS prints.

The member galaxies in SCGGs were initially described as being compact ("Compact Groups of Compact Galaxies"). Since they have relatively high surface brightness and usually lack diffuse borders (Shakhbazian 1973) they seemed to be compact on the POSS prints. Later studies showed, however, that the group members are mostly ordinary E or S0 galaxies. The impression of compact galaxies was strenghten due to contamination by foreground stars (Bettoni & Fasano 1993) in some groups in the original lists. However, recent spectral observations showed that contamination by stars is minimal (Tiersch et al., in preparation). Nevertheless, the original "compact" description of the member galaxies is no longer considered significant.

Being very dense, compact and flattened, the SCGGs are fruitful laboratories to study processes of dynamical friction, tidal interaction, collisions and galaxy merging. The SCGGs have attracted little attention until recently because they are more distant and fainter than HCGs. Indeed, although the redshifts of only a small sample (~ 50) of relatively bright SCGGs are known, a comparison of the redshift distributions (Fig. 1) shows that the median distance of SCGGs is at least three times larger than the median distance of HCGs. The redshifts of HCGs are taken from Hickson et al. (1988), and most redshifts for SCGGs are as yet unpublished data (Tiersch et al., in preparation). On the other hand the average flux density of HCGs at 60 μm is about 1.4 Jy, and the nominal threshold detection of the IRAS Faint Source Survey presented in the Faint Source Catalog (FSC) and Faint Source Catalog Regect (FSCR) is ~ 0.22 Jy. Therefore, assuming comparable FIR luminosity distributions of the galaxies in HCGs and SCGGs, FIR emission should be detectable by IRAS from SCGGs with the lowest redshifts or highest luminosities.

In this paper we report the results of a search for FIR emission from SCGGs using the IRAS archives. In Sect. 2 the IRAS data processing methods are reviewed; the results are presented in Sect. 3; and in Sect. 4 we briefly discuss the results and point out directions for future work.

2. The reduction of the IRAS data

The original SCGG lists (Shakhbazian 1973; Shakhbazian & Petrosian 1974; Baier et al. 1974; Petrosian 1974, 1978; Baier & Tiersch 1975, 1976a,b, 1978, 1979) contain 377 groups. In our study the groups Shkh 12, 78, 146, 180 and 275 were omitted because they have been found to contain mainly foreground stars. We were not able to reidentify four other groups (Shkh 206, 241, 301 and 353) since their positions in the original lists were incorrect. There was also one duplication (Shkh 214 = Shkh 252). Thus we searched for FIR emission in the IRAS archives at the positions of 367 SCGGs with accurate coordinates measured from the Digitized Sky Survey or other data (Stoll et al. 1993a,b, 1994a,b, 1996a,b,c, 1997a,b,c). The IRAS Point Source Catalog (PSC), the Faint Source Catalog (FSC) and the Faint Source Catalog Rejects (FSCR) were first searched for positional matches within SCGG boundaries. The fluxes of suspected weak sources with no cirrus contamination flags in the catalogs were measured using the Scan Processing and Integration (SCANPI) method of coadding the 1–dimensional IRAS scans (Helou et al. 1988). A detection was considered reliable if the FIR source was found within about 1 arcmin from the brightest galaxy in the group (consistent with the positional uncertainty ellipse from the FSC or FSCR), if one or more galaxies was found within the 60 μm IRAS beam, and if the signal to noise ratio (SNR) at 60 μm was larger than 4. The 60 μm IRAS band was by far the most sensitive for the detection of SCGGs, as for extragalactic objects in general. Full Resolution Coadded (FRESCO) images of 1 square degree fields were also examined for groups with candidate detections from the FSC, FSCR, or SCANPI. Since FRESCO images do not have the large-scale background removed (they are not point-source filtered), they provide additional information about the group environments, such as possible confusion due to nearby stars or Galactic cirrus.

In the SCANPI processing, the median of all acceptable scans was used to estimate the flux densities from each source. Most sources are weak point sources, and the flux density based on the template amplitude fit was used. In a few cases there were signs of slightly extended

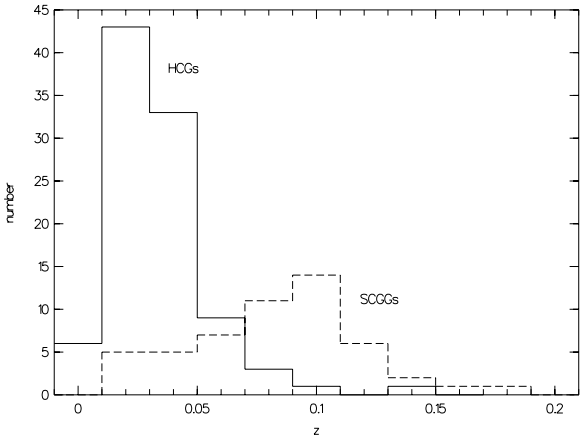

Fig. 1. Histograms of redshifts of HCGs and of SCGGs

emission, and the total flux within the beam area was used as the best estimator. In cases where a source is listed in the FSC or FSCR, SCANPI often provides a reliable 100 μm flux density estimate that is not in the catalogs.

3. Results

FIR sources were reliably detected at the positions of 24 out of the considered 367 SCGGs. Data for the detected FIR sources is presented in Table 1. Column 1 lists the Shakhbazian designation of the group in the first row. In the second row of Col. 1 the identification number of the galaxy (as labeled on the original SCGG finding charts) which is within the 60 μm IRAS beam and is suspected to be the dominant FIR emitter, based on proximity to the IRAS source position and optical brightness, is given. Column 2 gives the diameter of the group in arcminutes. In Cols. 3 and 4 the right ascension and declination (J2000.0) of the IRAS source are listed in the first row; the coordinates of the suspected dominant FIR-emitting galaxy are listed below. In Cols. 5, 6, and 7 the flux densities at 25 μm, 60 μm and 100 μm are presented together with their SNR (in parentheses). The fluxes determined by the SCANPI method in some cases differ from that given in the IRAS catalogs. This is generally due to underestimates of flux densities in the IRAS catalogs for sources which are slightly resolved by the IRAS beam.

Isophotes of the detected FIR sources at 60 μm overlaid on POSS[1] E (red) images of the groups are presented in Fig. 2. To produce these plots, the IRAS FRESCO/HIRES images in cartesian (nearly orthographic) B1950 coordinates were contoured into "vector files" in the B1950 system. Then the AGRA package developed at IPAC was used to project the contour vectors point-by point into the J2000 "plate" projection system of the DSS images. The reprojected contours were then overlayed on a grayscale of the J2000 DSS image, and a coordinate grid and scale were added using the IPAC Skyview image analysis package.

As mentioned above, the angular sizes of SCGGs are very small and in many cases they are of the order of $1-2$ arcmin. This is smaller than the angular resolution (beam size) of IRAS at 60 μm, which is nominally $5' \times 2'$ FWHM. Hence usually it is impossible to determine which galaxy of the group might be the dominant FIR emitter. It is likely, as suggested by Sulentic & De Mello Rabaça (1993) for HCGs, that more than one galaxy in the group contributes to the total observed FIR emission. In some cases, such as Shkh 22, 176 and 243, the FIR source is extended, providing evidence that more than one galaxy contributes to the FIR emission. The second IRAS source within the boundaries of Shkh 22 may be associated with galaxies No. 2 and/or 3. Thus, it is possible that in some cases IRAS has detected the integral FIR emission of a few galaxies in the groups.

Several IRAS sources were detected in the vicinity of SCGGs, but with positions and uncertainty ellipses centered outside the group boundaries. Most of these have been identified with galaxies or stars that are merely projected near the corresponding SCGGs. For 10 remaining SCGGs, IRAS sources were found close to the groups, but SCGG galaxy members could not be confidently identified as the FIR source for various reasons. The 10 SCGGs with possible IRAS detections are presented in Table 2, where the columns contain the same parameters as the first row in Table 1. Since the IRAS detector in-scan and cross-scan widths at 60 μm were $\sim$2.5 and $\sim$4 arcmin respectively, it is possible that these IRAS sources may be associated with members of the galaxy groups. However, confusion with foreground Galactic cirrus, lack of FSC or FSCR counterparts, or location near the edge of the IRAS beam make the identification very uncertain. The remarks following Table 2 indicate why each IRAS source has an uncertain association with the corresponding galaxy group. Figure 3 presents IRAS isophotes overlayed on visual DSS fields for the sources in Table 2.

4. Discussion

The percentage of SCGGs with confident FIR detections ($\sim$7%) is appreciably less than in HCGs (64%). One reason for the smaller percentage of FIR detections among Shakhbazian groups is probably their large distances. The median redshift of extragalactic objects selected by their 60 μm IRAS emission is $z = 0.03$ (Kleinmann & Keel 1987). This corresponds to a median FIR luminosity of $\sim 2\ 10^{10} L_{\odot}$. Among the sample of $\sim$ 50 Shakhbazian groups investigated spectroscopically to date, only 5 groups have $z \leq 0.03$, and the median redshift is $z = 0.0825$. Thus only relatively strong FIR sources with luminosity above $\sim 10^{11} L_{\odot}$ are detectable at these redshifts. The redshifts of only 4 Shakhbazian groups (Shkh 16, 331, 344, and 351) with detected FIR emission are known. These groups have 60 μm luminosities comparable to the most luminous HCGs.

What type of objects could be responsible for the observed FIR emission in SCGGs? A dominant population in HCGs are E/S0 galaxies, that are known to be very weak FIR emitters compared to later Hubble types (de Jong et al. 1984). Galaxy-galaxy interactions

[1] The images of the SCGGs were obtained using the photographs of the National Geographic Society-Palomar Observatory Sky Survey (NGS-POSS) obtained with the Oschin Telescope on Palomar Mountain. The NGS-POSS was founded by a grant from the National Geographic Society to the California Institute of Technology. The plates were processed into the present compressed digital form with their permission. The Digitized Sky Survey (DSS) was produced at the Space Telescope Science Institute under US Government grant NAG W-2166.

involving close, penetrating collisions, which are expected to be frequent in compact groups, are believed to trigger star formation processes or non-thermal nuclear activity associated with Seyfert nuclei. The latter are often associated with strong far-infrared flux (Antonucci & Olszewski 1985, 1986; Aaronson & Olszewski 1984) and they are believed to be the main source of FIR emission in dense groups. Even galaxies with mild activity according to the Byurakan classification of galaxies (Kalloglian & Tovmassian 1964) are relatively strong FIR emitters (Tovmassian 1994). At the same time, it is known that starburst and Seyfert galaxies are relatively blue objects. Unfortunately, at present there is insufficient photometric data on the Shakhbazian groups to determine whether groups with detected FIR emission contain bluer galaxies on average than those undetected by IRAS.

Recent searchers for signatures of tidal interactions and merging in the early-type galaxies that dominate HCGs (Zepf et al. 1991, Bettoni & Fasano 1993; Zepf 1993; Whitmore et al. 1993; Fasano & Bettoni 1994) have found that very few elliptical galaxies in HCGs have colors indicating recent star formation. In addition, the morphologies of galaxies in HCGs reveal only moderate evidence for tidal interactions and few clear cases of merging. Moles et al. (1994) made an extensive UBV photometry for 177 galaxies in HCGs and concluded that the star formation rate in these groups is only weakly enhanced compared to isolated galaxies. Moreover, Pildis et al. (1995) stressed that a straightforward explanation of the interaction history of HCGs is rather difficult. In addition, Kennicutt et al. (1987) showed that interaction-enhanced star formation is only a marginal effect in optically selected samples, while interactions are more significant in FIR-selected galaxy samples.

Proceeding from the morphological types of the constituent galaxies, N-body simulations suggest that Shakhbazian groups are a longer-lasting and more evolved type of system than the HCGs. Indeed, SCGGs contain on average a higher percentage of E's and S0's than the HCGs. While E and S0 galaxies comprise about 51% of galaxies in HCGs (Hickson et al. 1989), the fraction of E/S0 galaxies in a sample of 243 galaxies in SCGGs is 77% (Tiersch et al. 1996b). Thus the fraction of spirals, which have higher FIR luminosity for a given optical luminosity than E and S0 galaxies, is smaller among SCGGs than in the HCGs. It is remarkable that FIR emission was detected from only two (Shkh 16 and 351) out of 10 SCGGs with $z \sim 0.05$, while about half of HCGs at these redshifts has detectable FIR emission. Another possibility is that in the dense environments of SCGGs the gas and dust in disk galaxies may be swept out after numerous encounters. This, combined with the greater distances of SCGGs would explain their low IRAS detection rate compared to HCGs.

Recent studies (Tiersch et al. 1997) show that a significant fraction of Shakhbazian groups contain emission-line objects, including some Seyfert galaxies. Emission-line galaxies have been found in approximately one third (12 out of 36) of SCGGs which have been investigated spectroscopically to date. Assuming that this fraction is typical also for the SCGGs detected by IRAS (which do not yet have spectral data), and assuming that about 50% of Seyfert galaxies have 60 μm luminosities in excess of $\sim 10^{10} L_{\odot}$ (Miley et al. 1985), using the above mentioned approximate limit of detectability at the typical redshifts of SCGGs ($L_{\rm FIR} \sim 10^{11} L_{\odot}$), the FIR detection fraction of $\sim$7% for SCGGs may be explained by gas-rich newcomers falling from the outskirts of the groups into their inner region, where strong gravitational interactions result in star formation and enhanced FIR luminosity.

A number of SCGGs with IRAS detections also have radio continuum emission, which is generally characteristic of AGNs. Some SCGGs have an X-ray counterpart that may be due to the AGN of a corresponding galaxy in the group, or, more likely, to a hot intracluster gas (Tiersch et al. 1996a).

Future work should include spectroscopic observations of members of Shakhbazian groups, especially those with detected IRAS emission, in order to determine their distances, velocity dispersion, masses, luminosities, colors and other properties.

Acknowledgements. HMT and GHT are grateful to IPAC and JPL for financial support during the work at the IPAC, and to C. Beichman for hospitality. HMT was supported by the CONACYT research grant No. 5-000PE and by the DAAD. JMM was supported by the Jet Propulsion Laboratory, California Institute of Technology, under contract with NASA. HT is grateful to the Government of the land Brandenburg for the support of this work and DS acknowledges the support of the Deutsche Forschungsgemeinschaft, DFG project number TI 215/7-1.

References

Aaronson M., Olszewski E.W., 1984, Nat 309, 414
Allam S., Assendorp R., Longo G., Braun M., Richter G.M., 1996, A&AS 117, 39
Amirkhanian A.S., 1989, Soob. Byurakan Obs. 61, 27
Antonucci R.J., Olszewski E.W., 1985, AJ 90, 2203
Antonucci R.J., Olszewski E.W., 1986, AJ 91, 56
Baier F.W., Petrosian M.B., Tiersch H., Shakhbazian R.K., 1974, Afz 10, 327
Baier F.W., Tiersch H., 1975, Afz 11, 221
Baier F.W., Tiersch H., 1976a, Afz 12, 7
Baier F.W., Tiersch H., 1976b, Afz 12, 409
Baier F.W., Tiersch H., 1978, Afz 14, 279
Baier F.W., Tiersch H., 1979, Afz 15, 33
Becker R.H., White R., Helfand D.J., 1995, ApJ 450, 559
Bettoni D., Fasano G., 1993, AJ 105, 1291
Bontekoe T.R., Koper E., Kester D.J.M., 1994, A&A 284, 1037
Bushouse H.A., 1987, ApJ 320, 49
Douglas J.N., Bash F.N., Bozyan F.A., Torrence G.W., Wolfe C., 1996, AJ 111, 1945
Fasano G., Bettoni D., 1994, AJ 107, 1649

Gregory P.C., Condon J.J., 1991, ApJS 75, 1011
Hales S.E.G., Waldram E.M., Rees N., Warner P.J., 1995, MNRAS 274, 447
Helou G., Khan I., Malek L., Boechmer L., 1988, ApJS 68, 151
Hickson P., 1982, ApJ 255, 382
Hickson P., Kindl E., Huchra J.P., 1988, ApJ 331, 64
Hickson P., Menon T. K., Palumbo G.G.C., Persic M., 1989, ApJ 341, 679
Jong T. de, Clegg P.E., Soifer B.T., Rowan-Robinson M., et al., 1984, ApJ 278, L67
Joseph R.D., Wright G.S., 1985, MNRAS 214, 87
Kalloglian A.T., Tovmassian H.M., 1964, Contr. Byurakan Obs. 36, 32
Kennicutt Jr R.C., Keel W.C., van de Hulst J.M., Hummel E., Roettiger K.A., 1987, AJ 93, 1011
Kleinmann S.G., Keel W., 1987, in: Persson C. (ed.): Star Formation in Galaxies, Washington DC: US Govt. Print. Off., p. 559
Kodaira K., Sekiguchi M., Sugai H., Doi M., 1991, PASJ 43, 169
Laurikainen E., Moles M., 1989, ApJ 345, 176
Mathewson D.S., Ford V.L., 1996, ApJS 107, 97
Miley G.K., Neugebauer G., Soifer B.T., 1985, ApJ 278, L79
Moles M., Olmo A. del, Perea J., Masegosa J., Marquez I., Costa V., 1994, A&A 285, 404
Norman, C.A., 1988, in: Ruritz R., Fich M. (eds.): Galactic and Extragalactic Star Formation. Dordrecht, D. Reidel
Oleak H., Stoll D., Tiersch H., MacGillivray H.T., 1995, AJ 109, 1485
Petrosian M.B., 1974, Afz 10, 471
Petrosian M.B., 1978, Afz 14, 631
Pildis R.A., Bregman J.N., Schombert J.M., 1995, AJ 110, 1498
Sanders D.B., Soifer B.T., Elias J.H., Madore B.F., Matthews K., Neugebauer G., Scoville N.Z., 1988, ApJ 325, 74
Shakhbazian R.K., 1973, Afz 9, 495
Shakhbazian R.K., Petrosian M.B., 1974, Afz 10, 13
Stoll D., Tiersch H., Oleak H., Baier F., MacGillivray H.T., 1993a, Astron. Nachr. 314, 225
Stoll D., Tiersch H., Oleak H., Baier F., MacGillivray H.T., 1993b, Astron. Nachr. 314, 317
Stoll D., Tiersch H., Oleak H., MacGillivray H.T., 1994a, Astron. Nachr. 315, 11
Stoll D., Tiersch H., Oleak H., MacGillivray H.T., 1994b, Astron. Nachr. 315, 97
Stoll D., Tiersch H., Braun, M., 1996a, Astron. Nachr. 317, 239
Stoll D., Tiersch H., Braun, M., 1996b, Astron. Nachr. 317, 315
Stoll D., Tiersch H., Braun, M., 1996c, Astron. Nachr. 317, 369
Stoll D., Tiersch H., Cordis L., 1997a, Astron. Nachr. 318, 7
Stoll D., Tiersch H., Cordis L., 1997b, Astron. Nachr. 318, 89
Stoll D., Tiersch H., Cordis L., 1997c, Astron. Nachr. 318, 149
Sulentic J.W., De Mello Rabaça D.F., 1993, ApJ 410, 520
Tiersch H., Oleak H., Stoll D., Böhringer H., 1994, in: MacGillivray H.T. et al. (eds.) Astronomy from Wide-Field Imaging, IAU Symp. 161. Kluwer, Dordrecht, Boston, London, p. 623
Tiersch H., Oleak H., Stoll D., Schwope A.D., Neizvestny S., Böhringer H., MacGillivray H.T., 1996a, Max-Planck-Report 261, 125
Tiersch H., Stoll D., Neizvestny S., Tovmassian H.M., Navarro S., 1996b, J. Korean Astron. Soc. 29, 59
Tiersch H., Oleak H., Stoll D., Neizvestny S., Amirkhanian A.S., Egikian A.G., 1997, Afz (in print)
Tovmassian H.M., 1994, ApJ 430, 139
Veilleux S., Kim D.-S., Sanders D.B., Mazzarella J.M., Soifer B.T., 1995, ApJS 98, 171
Visser A.E., Riley J.M., Rottgering H.J.A., Waldram E.M., 1995, A&AS 110, 419
White R.L., Becker R.H., 1992, ApJS 79, 331
Whitmore B.C., Gilmore D.M., Jones C., 1993, ApJ 407, 489
Zepf S.E., 1993, ApJ 407, 448
Zepf S.E., Whitmore B.C., Levison H.F., 1991, ApJ 383, 524

Table 1. IRAS sources detected at the position of SCGGs

Shkh *Gal*	D [′]	RA (J2000) h m s	Dec (J2000) ° ′ ″	25 μm (SNR) (Jy)	60 μm (SNR) (Jy)	100 μm (SNR) (Jy)
013	1.8	16 45 18.4	53 42 44	<0.07	0.30 (8.9)	0.86 (3.7)
1		16 45 18.8	53 42 41			
014	0.9	14 25 20.0	47 15 28	<0.06	0.16 (3.7)	0.40 (5.5)
2		14 25 20.3	47 15 33			
016	5.0	16 49 13.4	53 24 30	<0.06	0.22 (8.5)	0.85 (7.2)
3		16 49 12.3	53 24 18			
022	1.5	15 45 48.9	55 06 33	<0.05	0.10 (5.8)	0.37 (7.4)
4		15 45 47.9	55 06 31			
063	0.9	11 29 33.5	42 26 36	<0.13	0.18 (5.6)	0.22: (3.3)
1		11 29 36.0	42 26 25			
065	4.0	11 30 55.8	35 01 03	<0.14	0.20 (8.5)	0.35 (3.8)
27		11 30 55.0	35 01 06			
074	4.2	14 20 54.3	43 03 24	<0.08	0.15 (7.3)	0.61 (3.8)
9		14 20 55.1	43 03 32			
104	1.2	09 27 14.9	52 58 29	<0.07	0.15 (3.9)	0.34 (3.5)
2		09 27 13.2	52 58 43			
135	2.4	16 13 26.3	64 21 25	<0.05	0.27 (12.5)	0.38 (6.3)
1		16 13 25.5	64 21 32			
168	3.3	18 27 31.7	83 06 04	<0.03	0.16 (11.7)	0.52 (4.6)
1		18 27 34.5	83 06 03			
176	1.0	00 08 17.8	29 59 21	<0.56	0.74 (15.0)	1.60 (12.8)
1		00 08 21.1	29 59 18			
243	3.9	12 09 31.3	32 24 48	<0.11	0.13 (4.5)	0.72 (5.2)
7		12 09 32.8	32 24 31			
248	1.3	13 12 14.2	36 11 03	<0.14	0.28 (9.7)	0.93 (9.5)
4		13 12 15.6	36 11 12			
251	3.2	13 36 50.7	36 50 22	<0.09	0.28 (9.5)	<0.32
2		13 36 50.9	36 50 20			
254	3.3	13 56 19.9	35 11 36	<0.08	0.15 (3.0)	0.53 (4.6)
3		13 56 19.0	35 11 20			
257	2.7	14 46 57.2	37 33 02	<0.06	0.17 (7.0)	0.46 (5.9)
1		14 46 55.3	37 33 20			
270	4.0	02 08 42.0	-13 57 33	<0.16	0.22 (7.5)	0.55 (7.8)
1		02 08 42.2	-13 58 07			
273	3.1	02 52 37.1	-13 06 09	0.15 (5.0)	0.37 (10.4)	1.01 (10.4)
3		02 52 36.0	-13 06 09			
310	2.2	00 54 51.8	-03 43 22	<0.14	0.40 (12.3)	0.91 (3.8)
3		00 54 51.6	-03 43 09			
331	1.1	22 25 29.0	-02 46 51	<0.12	0.17 (3.8)	0.41 (2.9)
7		22 25 26.8	-02 47 02			
344	2.9	08 47 37.3	03 42 09	<0.11	0.32 (4.5)	0.75 (9.6)
1		08 47 32.4	03 42 08			
351	2.5	11 10 24.5	04 49 43	<0.15	1.04 (25.3)	3.27 (26.7)
6		11 10 24.7	04 49 47			
371	0.9	11 43 30.4	21 54 27	<0.16	0.42 (8.8)	1.12 (9.4)
2		11 43 32.8	21 54 05			
376	1.9	13 56 35.9	23 21 40	0.25 (3.5)	0.20 (6.5)	0.76 (7.9)
4		13 56 35.7	23 21 37			

Remarks to Table 1:

In the remarks below, F designates IRAS Faint Source Catalog sources, and Z designates Faint Source Catalog Reject sources.

Shkh 013. F16441+5348. SCANPI shows source confusion at 100 μm peaked about $-4'$ in the in-scan direction. FRESCO confirms foreground confusion at 100 μm. Therefore FSC flux densities are used. May be combined emission of very close galaxies 1 and 2.

Shkh 014. F14234+4729. SCANPI template amplitude measurements used: confirms $S(60\ \mu\mathrm{m})$ from FSC, and adds a reliable $S(100\ \mu\mathrm{m})$ detection. May be combined emission of bright galaxies 2, 3, 5 and 6.

Shkh 016. F16480+5329. SCANPI at the position of F16480+5329 reproduces the FSC estimate at 60 μm, but adds a reliable 100 μm detection. May be combined emission of galaxies 1, 2 and 3. Galaxy 3 is closest. The group is known also as I Zw 167 and Arp 330. $z = 0.02913$ (Amirkhanian 1989). A radio source was observed at the position of the galaxy 1 (Gregory & Condon 1991; White & Becker 1992; Visser et al. 1995; Douglas et al. 1996).

Shkh 022. Z15445+5515. SCANPI confirms FSCR 60 μm measurement and adds reliable 100 μm detection at position of Z15445+5515. May be integrated emission of galaxy pair 4 and 5.

Shkh 063. Z11268+4243. SCANPI flux densities at the position of Z11268+4243 are used here.

Shkh 065. Z11282+3517. The FIR source coincides with galaxy 27. SCANPI flux densities at the position of the FSCR source are listed; SCANPI confirms $S(60\ \mu\mathrm{m})$ from the FSCR and adds an estimate for $S(100\ \mu\mathrm{m})$. It has a radio counterpart FIRST J113055.0+350104 (Becker et al. 1995). The group is identical with the cluster of galaxies A 1284.

Shkh 074. F14189+4317. SCANPI estimates at the position of the FSC source are listed. SCANPI $S(60\ \mu\mathrm{m})$ agrees with the FSC within the uncertainties, and SCANPI provides an estimate for $S(100\ \mu\mathrm{m})$. The IRAS source is associated with the eastern subgroup.

Shkh 104. Z09236+5311. SCANPI flux densities at position of the FSCR source are listed here. $S(60\ \mu\mathrm{m})$ agrees with the FSC within the uncertainties, and SCANPI provides an estimate for $S(100\ \mu\mathrm{m})$. May be combined emission of galaxies 2 and 3.

Shkh 135. F16129+6428. SCANPI fluxes at the position of the FSC source are listed.

Shkh 168. Z18340+8303. SCANPI fluxes at the position of the FSCR source are listed. Galaxies 1, 3, 4 and 5 are located in the central area of isophots. The radio source 8C 1834+830 (Hales et al. 1995) is at RA=$18^{\mathrm{h}}\ 27^{\mathrm{m}}\ 56\overset{\mathrm{s}}{.}5$, Dec= $83°05'55''$, at a distance of 0.3 arcmin from galaxies 5 and 6.

Shkh 176. F00057+2942. SCANPI fluxes at the position of the FSCR source are listed. May be combined emission of galaxies 1 and 4. Galaxies 5 and 9 are located nearby.

Shkh 243. SCANPI measurements are listed here. A source size larger than the IRAS 100 μm beam, very cool color temperature, and lack of a FSC or FSCR counterpart suggest this is possibly Galactic cirrus. The FIR source may be galaxy 7. The radio source FIRST J120932.9+322541 (Becker et al. 1995) is at about 1 arcmin from galaxy 7.

Shkh 248. F13099+3626. SCANPI measurements at the position of the FSC source are listed here. The nearest galaxy to the center of isophots is the brightest galaxy 4. Galaxies 1, 3, 5 and 8 are nearby. The radio source FIRST J131213.1+361311 (Becker et al. 1995) is at about 2 arcmin from galaxy 4.

Shkh 251. F13346+3705. SCANPI measurements at the position of the FSC source are listed here. May be combined emission of galaxies 1 and 2. The radio source FIRST J133647.3+364948 (Becker et al. 1995) is at about 1 arcmin from the mentioned pair of galaxies.

Shkh 254. Z13541+3526. SCANPI measurements at the position of the FSCR source are listed here. Galaxy 3 is the closest to the center of isophots. Nearby are galaxies 1, 7, 8, 9 and 10. The radio source FIRST J135619.1+351119 (Becker et al. 1995) is at the position of galaxy 3.

Shkh 257. F14449+3745. SCANPI measurements at the position of the FSC source are listed here; SCANPI confirms $S(60\ \mu\mathrm{m})$ from the FSC and adds a reliable $S(100\ \mu\mathrm{m})$ measurement. May be combined emission of galaxies 1 and 6.

Shkh 270. F02062−1411. SCANPI measurements at the position of the FSC source are listed here. SCANPI and FRESCO suggest a point source embedded behind Galactic cirrus. The brightest galaxy 1, and also galaxy 2 are closest to the center of isophots.

Shkh 273. F02505−1318. SCANPI measurements at the position of the FSC source are listed here. May be combined emission of galaxies 3, 5 and 6. Nearby are galaxies 2 and 4.

Shkh 310. F00523−0359. SCANPI measurements at the position of the FSC source are listed here. Galaxy 3 is in the center of isophots. Galaxies 1, 2, 4, 5 and 6 are located nearby.

Shkh 331. Z22228−0302. SCANPI measurements at the position of the FSCR source are listed here. The brightest galaxy 7 of the group together with closest galaxies 3, 4 and 5 are located in the center of isophots.

Shkh 344. Z08450+0353. SCANPI measurements at the position of the FSCR source are listed here. $z = 0.0782$ (Tiersch et al., in preparation) Galaxy 1 is the closest to the center of isophots. Galaxies 3, 4 and 7 are located neraby.

Shkh 351. F11078+0505. SCANPI measurements at the position of the FSC source are listed here. The source is identified with the brightest galaxy 6 (UGC 06212), located in the center of isophots. It has the same $z = 0.030$ (Mathewson & Ford 1996), as other galaxies of the group (Kodaira et al. 1991, and Tiersch et al., in preparation). SCANPI shows a very weak source with $S(60\ \mu)\sim 0.3$ Jy about $2.5'$ from the bright peak of F11078+0505. This corresponds to the distorted FRESCO contours at this location (Fig. 2), and may represent emission associated with galaxy 4 or 5 in Shkh 351.

Shkh 371. F11409+2211. SCANPI measurements at the position of the FSC source are listed here. All 5 galaxies of this very compact group are located in the central area of isophots.

Shkh 376. Z13542+2336. SCANPI measurements at the position of the FSCR source are listed here. The extended 60 μm and 100 μm emission and cool color temperature suggest possible cirrus confusion.

Table 2. IRAS Sources with uncertain SCGG Associations

Shkh	D [′]	RA (J2000) h m s	Dec (J2000) ° ′ ″	25 μm (SNR) (Jy)	60 μm (SNR) (Jy)	100 μm (SNR) (Jy)
006	1.7	11 18 40.7	51 43 27	<0.11	0.33 (7.7)	0.67 (6.4)
008	0.6	16 03 45.9	52 21 26	<0.05	0.13 (5.9)	0.31 (3.7)
030	5.0	23 47 25.2	−02 19 00	<0.17	0.37 (5.4)	0.59 (5.5)
113	1.3	10 21 05.5	61 12 04	<0.10	<0.12	<0.35
120	2.9	11 04 33.5	35 52 15	<0.08	0.25 (5.8)	0.55 (2.8)
131	3.2	14 38 13.5	62 41 49	<0.08	0.55 (14.3)	1.32 (10)
218	3.0	14 33 38.4	26 41 27	<0.24	0.10 (3.0)	0.41 (4.2)
244	2.3	12 17 14.6	35 18 14	<0.08	0.20 (5.1)	<0.45
326	1.9	13 31 23.0	−08 22 39	<0.20	0.19 (4.7)	0.88 (5.6)
354	2.3	13 02 44.3	03 19 44	<0.20	0.55 (9.7)	1.51 (11.1)

Remarks to Table 2:

Shkh 006. F11158+5159 is about 1.5′ SW from the group. The large distance from the group in the in-scan direction make association unlikely. SCANPI measurements listed, providing a reliable 100 μm detection; $S(60\ \mu\mathrm{m})$ agrees with FSC within errors.

Shkh 008. Z16024+5229 is near galaxy 1. SCANPI measurements listed; use of template amplitude (tmp) fit omits flux from nearby confusing source. SCANPI also provides a reliable $S(100\ \mu\mathrm{m})$, that the FSCR does not, and agrees well with FSCR at 25 and 60 μm. Uncertainty in association is because FRESCO suggests that the weak 60 μm point-source could be confused by large-scale emission from two bright Galactic cirrus or molecular clouds on each side of the group (cf. Fig. 3).

Shkh 030. Coincides with HCG 97. $z = 0.0218$ (Hickson et al. 1988; Amirkhanian 1989). SCANPI shows a weak extended source at 60 μm centered at the given position; an extended 100 μm source is centered 2′ away, suggesting foreground confusion. The lack of IRAS FSC or FSCR counterparts, or a FIRST radio continuum source, make this IRAS association very uncertain.

Shkh 113. The source located about 3′ NE from the galaxy group is F10180+6128; it has $S(60\ \mu\mathrm{m})=$ 0.56 Jy. The weak source coincident with the position of Shkh 113 in the 60 μm FRESCO image (Fig. 3) also appears as a distinct object with SCANPI. However, the total flux within the zero-crossings of the baseline fit (−0.9′ to 0.8′) at the position of galaxy 1 is only $S(60\ \mu\mathrm{m})$=0.06 Jy; this is less than a 2σ signal, so upper limits at the position of galaxy 1 are listed here.

Shkh 120. The 60 μm emission in the FRESCO image peaks near galaxy 4. The lack of a corresponding source in the FSC or FSCR, extended nature of the emission in FRESCO, offsets in the centroids of the 60 μm and 100 μm emission, and large-scale correlated noise visible with SCANPI suggests this is foreground cirrus emission. The FIRST radio source J110433.1+355222 (Becker et al. 1995) coinsides with galaxy 4. The radio source is registered also in Gregory & Condon (1991).

Shkh 131. Fluxes listed are from the FSC for F14370+6254, centered about 1′ south of the group. This is the source at the center of the FRESCO isophotes in Fig. 3. SCANPI does not show a source distinct from F14370+6254; Shkh 131 is located near the edge of the 60 μm beam.

Shkh 218. The source about 3′ SW of the galaxy group is Z14312+2654. SCANPI shows a double source separated by 3′ at 60 μm; the NW component is the weak source at the location of the galaxy group (see Fig. 3). Flux density estimates listed here are from SCANPI; they are uncertain because of the lack of a FSC or FSCR counterpart, and possible cirrus confusion.

Shkh 244. The FRESCO 60 μm image shows an extended double structure in the east-west direction, and the 100 μm SCANPI data suggest possible cirrus. A 60 μm-only detection with no FSC or FSCR entry is always suspect for a faint point source. The radio source FIRST J121710.9+351757 (Becker et al. 1995) is very close (<1 arcmin) from galaxy 4.

Shkh 326. SCANPI measurements are listed. The source is not in the FSC or FSCR, and appears in SCANPI as a weak extended source. The color temperature and extended 60 μm and 100 μm emission suggest cirrus confusion.

Shkh 354. F13001+0335. SCANPI measurements at the position of the FSC source are listed here. The 60 μm and 100 μm profiles are slightly extended, and the large distance from any Shkh 354 galaxy makes the IRAS association with the group Shkh 354 highly uncertain. The DSS image shows another faint source much closer to the FSR positional uncertainty ellipse.